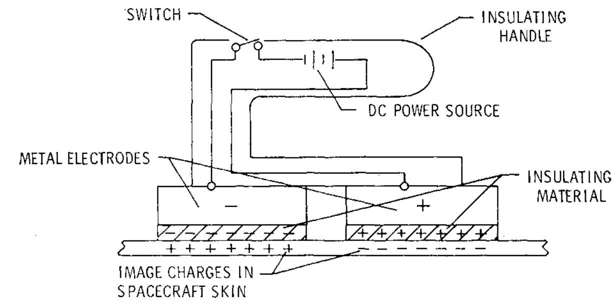

Fig. 3 Two-pole electroadhesor.

definition of electroadhesion and the construction of several prototype electroadhesors. Figure 3 is a sketch of an electroadhesive handhold. In the prototype devices, the high voltages required were obtained from a solid state oscillator (powered by ordinary pen light batteries) whose voltage was increased by a transformer then rectified by a solid state voltage doubler. The device in Fig. 3 is bipolar, consisting of two coated plates which become oppositely charged upon application of power. Then these plates contact a conducting surface, they impress upon the surface an electric field which produces migration of charges within the surface such that charges of a given polarity in the electroadhesor line up with charges of opposite polarity in the surface. The forces of attraction between these opposing charges produce the adhesion. The theory of electroadhesion and the study contract results are reported in Ref. 1.

Contracts for related work in electroadhesion were let by Marshall Space Flight Center and Wright-Patterson Air Force Base (WPAFB). No new information was reported.

LRC Electroadhesor Evaluation Program

The development of electroadhesors is dependent on the requirements of the particular applications. Thus, the development of electroadhesors requires much basic research. Such research determines the characteristics and capabilities of practical electroadhesive devices. Simulation of typical tasks determine the required characteristics. Concurrent with the simulation studies, actual electroadhesors must be developed having the characteristics found necessary in the simulation studies. Following these studies, spaceflight verification is required before electroadhesors become operational tools.

LRC is presently conducting the following two basic programs to determine the task requirements and electroadhesor capabilities.

1. I/EVA task requirements

A simulation study to investigate the characteristics (force levels, torques, etc.) of a series of I/EVA tasks representative of those expected in future space missions has been initiated. The simulation studies will be conducted in the LRC water-immersion simulation facility, and all tests will utilize electromagnets for attachment. Electromagnets simulate, to a large degree, electroadhesors and can be designed to provide a wide range of force levels and configurations. The tasks to be evaluated will primarily consist of: 1) astronaut maneuvering using handholds, shoes, and handrails; and 2) cargo transfer for packages having various sizes and masses and varying handhold locations. The tests will be conducted both with and without pressure suits.

Preliminary studies to develop electromagnet hardware have been initiated and have produced representative electromagnets for use as handholds and shoes. Initial indications in the cargo-handling studies are that the capability to move handholds to various locations on the package during transfer has a large advantage over a fixed position handhold, in that it permits variations in box c.g. location and varying control of package during transfer.

2. Electroadhesor hardware evaluation

The LRC contract provided basic experimentation to determine electroadhesor capabilities, and factors that influence the electroadhesive phenomenon and to develop prototype devices. LRC inhouse work has consisted of enhancing the electroadhesive devices obtained from Chrysler by increasing the voltage, varying the insulating material and method of introducing charges to the spacecraft surface and changing mechanical configuration to meet operational considerations. Several devices representative of two methods being used to produce the electrostatic field were constructed. These included bipolar devices evolving from the concept shown in Fig. 3 as well as those which directly introduced a d.c. ground to the conductive surface through the use of pins. Both devices utilize a thin sheet of insulating material on their bases. These devices are being evaluated.

Concluding Remarks

Initial studies of the electroadhesive phenomenon have indicated that electroadhesors are potentially usable as zero-g assistive devices for a range of intra- and extravehicular activities. These uses generally are related to astronaut and cargo maneuvering, worksite restraint and tool and equipment tiedown. Further studies are required to completely define the capabilities and applicability of electroadhesors.

References

[1] Krape, R. P., "Applications Study of Electroadhesive Devices," NASA CR-1211, Oct. 1968, Chrysler Corp. Space Div., New Orleans, La.

Effect of Lift Variation on the Impact of a Rolling Re-Entry Vehicle

J. P. CRENSHAW*
The Aerospace Corporation, San Bernardino, Calif.

Nomenclature

A	= reference area, ft^2
$C(\ )$	= Fresnel's cosine integral [Eq. (12)]
C_D	= vehicle drag coefficient
$C_{L\alpha}$	= vehicle lift-coefficient-curve slope when $\alpha = 0$, deg^{-1}
CR	= crossrange, ft
DR	= downrange, ft
g	= gravitational acceleration, 32.2 ft/sec^2
h	= altitude, ft
I	= moment of inertia about the vehicle roll axis, slug-ft^2
P	= roll rate, rad/sec
R	= radius of the base of a conical surface of possible dispersed trajectories, ft
$S(\ )$	= Fresnel's sine integral [Eq. (12)]
t	= time, sec
V	= vehicle velocity, fps
W	= vehicle weight, lb
x, y, z	= moving coordinates
X, Y, Z	= Newtonian coordinates
α	= trim angle of attack, deg

Received October 26, 1971; revision received November 15, 1971.
* Member of the Technical Staff. Member AIAA.

β = ballistic coefficient W/C_DA, psf
γ = flight-path angle (negative quantity), rad
$\bar{\gamma}$ = mean flight-path angle defined by Eq. (2) (negative quantity), rad
δ = angular flight-path deflection, rad
ε = angle between the radius vector from the center of curvature of the motion produced by lift and the lift vector, rad
η = +1 for roll acceleration, −1 for roll deceleration [Eq. (16)]
θ = roll angle between the vehicle lift vector and the x axis, $\phi - \varepsilon$, rad
ρ = atmospheric density, slug/ft^3
ϕ = angle between the radius vector from the center of curvature of the motion produced by lift and the x axis, rad

Subscripts

a = beginning of a linear roll rate variation or lift step
av = average condition during roll rate variation
b = end of a linear roll rate variation
e = re-entry conditions
i,j = counting indices
id, Im = impact deviation and impact, respectively
max = maximum
n = total number of linear roll rate variations and/or lift steps
o = known conditions

Superscript

$(\dot{\ })$ = differentiation with respect to time

Introduction

THE influence of a constant lift force on the trajectory of a rolling re-entry vehicle has been discussed in Ref. 1 for vehicles with constant roll rate and for vehicles which experience a roll rate variation. The purpose of this Note is to extend that analysis to include the effect of simple step changes in lift, resulting from step changes in trim angle of attack, which occur over a small interval of time compared to that necessary for the vehicle to roll through one cycle. The motion of the center of gravity of a re-entry vehicle experiencing a lift and/or roll rate variation is illustrated in Fig. 1. In general, when such variation occurs, the lift will not be distributed evenly about the zero-lift flight path as is the case when the lift and the roll rate are both constant. A deviation of the actual impact point from the zero-lift impact point occurs as a result.

Discussion

The equations for the components of flight-path deviation in the x and y directions derived in Ref. 1 are

$$R_x = \left(\frac{g}{2}\right)\left[\frac{C_{L_\alpha}\alpha A}{W}\frac{\rho Vh}{\sin\bar{\gamma}}\right]_{av}\int_{t_a}^{t_b}\cos\theta dt - \left(\frac{g}{2}\right)\left[\frac{C_{L_\alpha}\alpha A}{W}\frac{\rho Vh}{\sin\bar{\gamma}}\frac{\sin\theta}{P}\right]_b + \left(\frac{g}{2}\right)\left[\frac{C_{L_\alpha}\alpha A}{W}\frac{\rho Vh}{\sin\bar{\gamma}}\frac{\sin\theta}{P}\right]_a \quad (1a)$$

$$R_y = -\left(\frac{g}{2}\right)\left[\frac{C_{L_\alpha}\alpha A}{W}\frac{\rho Vh}{\sin\bar{\gamma}}\right]_{av}\int_{t_a}^{t_b}\sin\theta dt - \left(\frac{g}{2}\right)\left[\frac{C_{L_\alpha}\alpha A}{W}\frac{\rho Vh}{\sin\bar{\gamma}}\frac{\cos\theta}{P}\right]_b + \left(\frac{g}{2}\right)\left[\frac{C_{L_\alpha}\alpha A}{W}\frac{\rho Vh}{\sin\bar{\gamma}}\frac{\cos\theta}{P}\right]_a \quad (1b)$$

Equations (1) were derived assuming a straight flight path (i.e., γ = const). However, these equations apply for slightly curved flight paths with $\bar{\gamma}$ derived from

$$1/\sin\bar{\gamma} = 1/h\int_0^h (1/\sin\gamma)\,dh \quad (2)$$

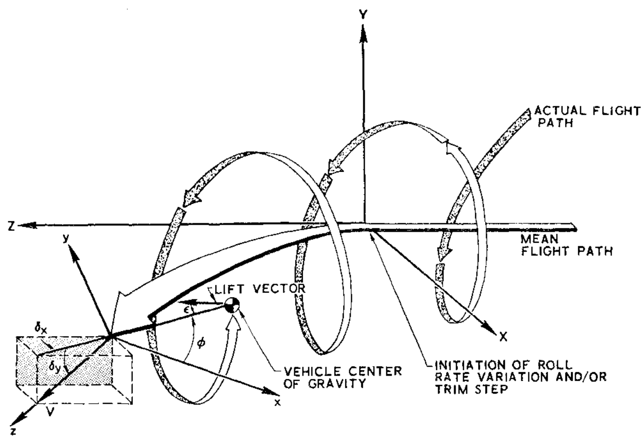

Fig. 1 Re-entry vehicle motion with a change in lift and/or roll rate.

The time interval $t_b - t_a$ includes the roll rate variation and, for the purpose of this analysis, t_a corresponds to the instant that the trim angle of attack changes. The maximum possible crossrange deviation at impact is

$$R = (CR)_{\max} = (R_x{}^2 + R_y{}^2)^{1/2} \quad (3)$$

and the maximum possible downrange deviation is

$$(DR)_{\max} = -R/\sin\gamma_{Im} \quad (4)$$

The roll angle (θ) is determined by integrating the roll equation

$$\ddot{\theta} = \dot{P} \quad (5)$$

where $\dot{P}$ is assumed to be constant over an increment of roll rate variation.

Lift Step with Constant Roll Rate

If the roll rate is constant then $\dot{P} = 0$ and the roll angle as a function of time is

$$\theta = \theta_0 + P_0(t - t_0) \quad (6)$$

where θ_0 is the roll angle at a specified time, t_0. Since the roll rate is constant, the integrals of Eqs. (1) are zero and the effect of a series of step changes in lift on impact can be expressed

$$R_x = -(g/2)\sum_{i=1}^{n}\{(C_{L_\alpha}A/W)(\rho Vh/\sin\bar{\gamma})[(\alpha_b - \alpha_a)/(P_0)]\sin\theta\}_i \quad (7a)$$

$$R_y = (g/2)\sum_{i=1}^{n}\{(C_{L_\alpha}A/W)(\rho Vh/\sin\bar{\gamma})[(\alpha_b - \alpha_a)/(P_0)]\cos\theta\}_i \quad (7b)$$

where the step changes in lift are the result of the step changes in trim angle of attack, $(\alpha_b - \alpha_a)_i$. Equations (7) in Eq. (3) yields the magnitude of the flight-path deflection distance at impact. For a single lift step this result is

$$R = -\frac{g}{2}\left[\left(\frac{C_{L_\alpha}A}{W}\right)\left(\frac{\rho Vh}{\sin\bar{\alpha}}\right)\right]_a\left|\frac{\alpha_b - \alpha_a}{P_0}\right| \quad (8)$$

Lift Step with Roll Rate Variation

The general result of Ref. 1 describes the effect of linear roll rate variation on the impact of a re-entry vehicle with a constant trim angle of attack. A more general form of this result, which describes the effect of step changes in trim angle of attack and linear variations of the roll rate on impact, can be obtained by integrating Eqs. (1) piecemeal between trim steps as well as between changes in roll acceleration. Interpreting i as a change in roll acceleration and/or a step change in trim angle of attack, this integration yields

$$R_x = g\sum_{i=1}^{n}\left\{\left[\frac{C_{L_\alpha}\alpha A}{W}\frac{\rho V h}{\sin\bar{\gamma}}\right]_{av}\frac{\Gamma}{|\dot{P}|^{1/2}}\cos\left[\sigma+\theta_a-\left(\frac{\pi}{2}\right)\eta t_a'^2\right]+\frac{1}{(2\pi^{1/2})}\left[\frac{C_{L_\alpha}\alpha A}{W}\frac{\rho V h}{\sin\bar{\gamma}}\right]_a\frac{1}{|\dot{P}|^{1/2}}\frac{\sin\theta_a}{t_a'}-\frac{1}{(2\pi^{1/2})}\left[\frac{C_{L_\alpha}\alpha A}{W}\frac{\rho V h}{\sin\bar{\gamma}}\right]_b\frac{1}{|\dot{P}|^{1/2}}\frac{\sin\theta_b}{t_b'}\right\}_i \quad (9a)$$

$$R_y = -g\sum_{i=1}^{n}\left\{\left[\frac{C_{L_\alpha}\alpha A}{W}\frac{\rho V h}{\sin\bar{\gamma}}\right]_{av}\frac{\Gamma}{|\dot{P}|^{1/2}}\sin\left[\sigma+\theta_a-\left(\frac{\pi}{2}\right)\eta t_a'^2\right]+\frac{1}{(2\pi^{1/2})}\left[\frac{C_{L_\alpha}\alpha A}{W}\frac{\rho V h}{\sin\bar{\gamma}}\right]_a\frac{1}{|\dot{P}|^{1/2}}\frac{\cos\theta_a}{t'_a}-\frac{1}{(2\pi^{1/2})}\left[\frac{C_{L_\alpha}\alpha A}{W}\frac{\rho V h}{\sin\bar{\gamma}}\right]_b\frac{1}{|\dot{P}|^{1/2}}\frac{\cos\theta_b}{t_b'}\right\}_i \quad (9b)$$

where

$$\Gamma_i = (\pi^{1/2}/2)\{[C(t_b') - C(t_a')]^2 + [S(t_b') - S(t_a')]^2\}_i^{1/2} \quad (10)$$

$$\sigma_i = \tan^{-1}\{[S(t_b') - S(t_a')]/(\eta[C(t_b') - C(t_a')])\}_i \quad (11)$$

$$C(t) = \int_0^t \cos\left[\left(\frac{\pi}{2}\right)x^2\right]dx,\ S(t) = \int_0^t \sin\left[\left(\frac{\pi}{2}\right)x^2\right]dx \quad (12)$$

$$(\theta_b)_i = (\theta_a)_i + \left(\frac{\pi}{2}\right)\sum_{j=1}^{i}[\eta(t_b'^2 - t_a'^2)]_j \quad (13)$$

$$(\theta_a)_i = (\theta_b)_{i-1} \quad (14)$$

$$(t_a')_i = \left(\frac{1}{\pi^{1/2}}\right)\left(\frac{P_a}{|\dot{P}|^{1/2}}\right)_i,\ (t_b')_i = \left(\frac{1}{\pi^{1/2}}\right)\left(\frac{P_b}{|\dot{P}|^{1/2}}\right)_i \quad (15)$$

$$\eta_i = (\dot{P}/|\dot{P}|)_i \quad (16)$$

Fresnel's integrals, defined by Eqs. (12), are tabulated in Ref. 2. The functions of Eqs. (10) and (11), which contain these integrals, are presented in Ref. 1 in terms of the roll rate boundary conditions.

An interesting special case of this result is the combined effect of discontinuities in both the roll rate and trim angle of attack. That is, infinite roll acceleration or deceleration between finite roll rate boundary conditions combined with a step change in trim at the same instant. This result is described by taking the limit of Eqs. (9) as $|\dot{P}| \to \infty$ and substituting into Eq. (3) to obtain

$$R = -\left(\frac{g}{2}\right)\left[\frac{C_{L_\alpha}A}{W}\left(\frac{\rho V h}{\sin\bar{\gamma}}\right)\right]_a\left|\frac{\alpha_b P_a - \alpha_a P_b}{P_a P_b}\right| \quad (17)$$

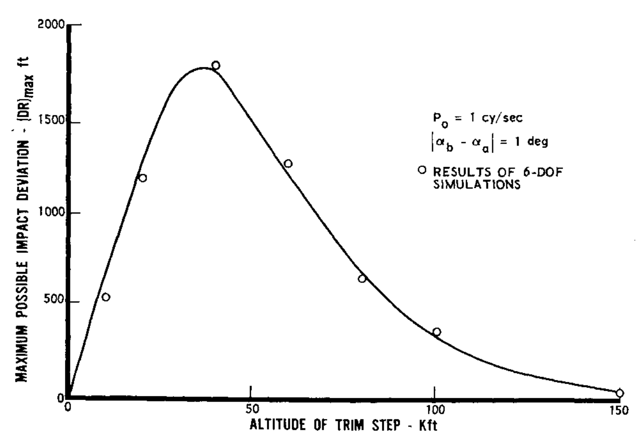

Fig. 2 Effect of a step change in lift on re-entry vehicle impact for constant roll rate.

Table 1 Combined Effect of a lift step and a roll rate variation from 1 cy/sec

Case	P_b, cy/sec	α_a, deg	α_b, deg	$[(DR)_{max}]_{Eq.\ 17}$, ft	$[(DR)_{max}]_{6\text{-}DOF}$ ft
1	$\frac{3}{2}$	0	1	1184	1126
2	2	0	1	888	856
3	3	0	1	592	605
4	$\frac{1}{2}$	0	1	3551	3304
5	$\frac{1}{2}$	$\frac{1}{2}$	1	2663	2493

Eq. (17) includes the result for constant roll rate as a special case since for $P_a = P_b$ this expression reduces to Eq. 8.

Results and Conclusions

An example of the effect of roll rate variation on the impact of a re-entry vehicle was presented in Ref. 1. That same vehicle will be used here to obtain an example of the effect of a trim step at constant roll rate on impact. The relevant physical characteristics of the vehicle are: $\beta = 2000$ psf, $W = 131$ lbs, $A = 0.92$ ft^2, and $C_{L_\alpha} = 0.034$ deg^{-1}. The re-entry velocity and flight-path angle are 22,690 fps and $-20°$, respectively. The effect of a one degree step change in trim angle of attack on impact at a constant roll rate of one cycle per second is shown in Fig. 2 as a function of the altitude at which the step occurs. These results were obtained using Eqs. (8) and (4). Included also are the results of six-degree-of-freedom trajectory simulations for comparison.

The results of Ref. 1 indicated that the effect of roll rate variation from one cycle per sec on impact for the vehicle and re-entry conditions described previously and for $|\dot{P}| \approx 50$ cy/sec^2 at an altitude of 35,000 ft were essentially the same as those for $|\dot{P}| \to \infty$ at the same altitude. Therefore, $|\dot{P}| \approx 50$ cy/sec^2 was used in various six-deg-of-freedom trajectory simulations of the combined effect of lift and roll rate variation, and compared to results using Eqs. (17) and (4) in Table 1. All of the results of this analysis compare well with the results from the trajectory simulations.

References

[1] Crenshaw, J. P., "Effect of Lift with Roll Rate Variation on Re-Entry Vehicle Impact," *Journal of Spacecraft and Rockets*, Vol. 8, No. 5, May 1971, pp. 483–488.

[2] Jahnke, E. and Emde, F., *Tables of Functions*, Dover, New York, 1945, pp. 34–37.

Ion Propulsion System: Regulation of the Vaporizer Temperature

C. Landrault* and M. Briot†

Laboratoire d'Automatique et de ses Applications Spatiales du C.N.R.S., Toulouse, France

Nomenclature

a = average radius of the ionizer pores
A = molecular mass of cesium
A_i = emitting area of the ionizer

Received August 3, 1971; revision received November 29, 1971.
Index category: Electric and Advanced Space Propulsion.
* Research Engineer, Ion Propulsion and Digital Technics Team.
† Dr. in Electronics, Ion Propulsion and Digital Technics Team.